ELSEVIER

PALAEO

Palaeogeography, Palaeoclimatology, Palaeoecology 204 (2004) 145–164

www.elsevier.com/locate/palaeo

Sea surface temperature variability in the North Atlantic during the last two glacial–interglacial cycles: comparison of faunal, oxygen isotopic, and Mg/Ca-derived records

E.S. Kandiano [a,*], H.A. Bauch [b], A. Müller [c]

[a] *GEOMAR, Wischhofstrasse 1–3, 24148 Kiel, Germany*
[b] *Mainz Academy of Sciences and Literature at GEOMAR, Wischhofstrasse 1–3, 24148 Kiel, Germany*
[c] *An der Tuchbleiche 9, 67240 Bobenheim–Roxheim, Germany*

Received 21 February 2003; received in revised form 9 October 2003; accepted 31 October 2003

Abstract

Climate variability in the northeast Atlantic was investigated on glacial–interglacial and millennial time scales during the last 200 000 years, using sea surface temperature (SST) records derived from planktonic foraminiferal diversities and from Mg/Ca measurements on *Globigerina bulloides*. Paleoceanographical interpretations are supported by species composition analyses, benthic and planktonic isotopic data as well as records of iceberg-rafted debris (IRD). Differences of climate development are recognized for both interglacial and glacial periods. Temperature estimates indicate slightly warmer conditions (up to 2°C) during marine oxygen isotope stage (MIS) 5e than during the Holocene. In contrast to the last glaciation, when the SST minimum coincided with a minimum in solar insolation immediately before Termination I, during the penultimate glaciation a long SST minimum occurred at times of intermediate solar insolation well preceding the onset of Termination II. This discrepancy between two glacial terminations may be explained by an inherently different orbital configuration characteristic for each glacial interval. Despite these differences between the two glacial trends, the superimposed shorter-lived climatic events reveal the same order of principal steps, implying their common causal nature. A direct comparison of faunal SSTs with those retrieved from Mg/Ca analysis shows that Mg/Ca-derived temperatures follow the general glacial–interglacial trend; however, the latter appear to be largely overestimated. Supported by $\delta^{18}O$ data in *G. bulloides*, which show little response to millennial-scale variability, there seems to be a need for species-dependent calibration experiments that also consider the different oceanographic settings this particular species can live in.

Keywords: Northeast Atlantic; climate variability; planktonic foraminifera; faunal SSTs; Mg/Ca SSTs

1. Introduction

According to recent concepts, variations in thermohaline circulation (THC) in the North Atlantic are regarded as the main mechanism that may amplify an initial impulse, thereby changing

* Corresponding author. Tel.: +49-431-6002848; Fax: +49-431-6002941.
E-mail address: ekandiano@geomar.de (E.S. Kandiano).

0031-0182/03/$ – see front matter © 2003 Elsevier B.V. All rights reserved.
doi:10.1016/S0031-0182(03)00728-4

climate into different modes (Broecker and Denton, 1990; Oppo and Lehmann, 1995; Rahmstorf, 1995). In turn, changes in THC occur when sea surface properties (e.g. salinity, temperature) for any current mode become distorted (Seidov and Maslin, 1999; Marotzke, 2000; Ganopolski and Rahmstorf, 2001; Clark et al., 2002). In this respect, sea surface temperatures (SSTs) are highly suitable for predicting future climate changes on the basis of modeling experiments. It is generally accepted that the method of planktonic foraminiferal census counts yields SST records that can be used successfully to reconstruct past climates (e.g. Imbrie and Kipp, 1971; Prell, 1985). More recently, emphasis has intensified to explore and to use geochemical methods such as Mg/Ca in foraminiferal tests in similar ways (Nürnberg et al., 2000; Elderfield and Ganssen, 2000; Pahnke et al., 2003). However, due to certain shortcomings inherent to each of the established SST methods, every new independent approach that can translate a paleotemperature signal is of great interest.

Since the first quantitative SST estimates based on faunal diversity in North Atlantic sediments revealed that the main glacial–interglacial pattern of the late Quaternary resulted from changes in orbital parameters (Ruddiman and McIntyre, 1976, 1984; Ruddiman et al., 1986a,b), a great deal of new information has been obtained which improved our knowledge of climate change during this period. It was discovered that abrupt, short-lived climate events are superimposed on the major glacial–interglacial trend. In Greenland ice cores they are recognized as Dansgaard–Oeschger cycles (e.g. Johnsen et al., 1992; Dansgaard et al., 1993; Grootes et al., 1993; Grootes and Stuiver, 1997), of which each terminates in a considerable cooling. The most severe of these cooling episodes are associated with ice sheet collapses and are identified in North Atlantic marine sediment records by enhanced occurrence of iceberg-rafted debris (IRD), material delivered during melting iceberg discharge, and a decrease in planktonic $\delta^{18}O$ due to meltwater input (Heinrich, 1988; Bond and Lotti, 1995; Bond et al., 1992, 1993). Until now, most of such detailed studies have concentrated on the last 130 ka. However, similar events with increased IRD input were also reported for the penultimate glaciation (Oppo and Lehmann, 1995; McManus et al., 1999; Didié and Bauch, 2000), but lack of SST reconstructions did not allow for an in-depth investigation of short-term climate variability during the penultimate glaciation or a more profound comparison of these two climate cycles.

Here we present paleotemperature records for the last two glacial–interglacial cycles inferred from foraminiferal census counts calculated with the modern analog technique (MAT) (Prell, 1985) and with the transfer function technique (TFT) (Imbrie and Kipp, 1971), showing how climate conditions changed on both long-term and millennial time scales during the last two glacial–interglacial cycles. The interpretation of the SST data sets is further supported by benthic and planktonic $\delta^{18}O$ measurements as well as IRD records. The results of these traditional approaches of SST estimations are used to test the first in the Northeast Atlantic temperature record derived from Mg/Ca measurements performed on *Globigerina bulloides*.

2. Materials and methods

2.1. Oceanographic setting, core location, and stratigraphy

Hydrographical changes in the North Atlantic region are mainly determined by the dynamics of the North Atlantic Drift (NAD). During warm periods like the present, the high-salinity Atlantic surface waters propagate to the cold Nordic seas where they gain density, thereby promoting the global ocean conveyor (Broecker and Denton, 1990). In glacial periods, ice sheets appeared around the Nordic seas and the surface ocean there became fresher due to iceberg melting. This freshwater prevented northward sea surface flow, causing a southward shift of the centers of deep water formation and an overall reduction of THC intensity (Duplessy et al., 1988; Ganopolski and Rahmstorf, 2001).

Gravity core M23414-9 (53.537°N, 20.288°W; water depth 2199 m), spliced together with trig-

ger-box core M23414-6 (53.537°N, 20.290°W; water depth 2201 m), was selected for the study. The selected site is directly influenced by the NAD (Fig. 1) and, moreover, is situated within the glacial IRD belt (Ruddiman, 1977; Grousset et al., 1993). Therefore, this location successfully captures glacial–interglacial as well as millennial-scale changes in NAD dynamics (Helmke et al., 2002). An additional advantage is that the selected core is located well above the lysocline during both glacial and interglacial times, which results in a good preservation of foraminiferal tests allowing accurate temperature reconstructions based on assemblage diversities.

The investigated section of M23414 goes back to late MIS 7. The stratigraphic subdivision of M23414 is based on planktonic and benthic oxygen isotope records, and on the centimeter-sampled lightness record. Ages were assigned according to the SPECMAP chronology (Helmke and Bauch, 2001; Helmke et al., 2002). The chronology of the uppermost section of M23414 is also supported by accelerator mass spectrometry ^{14}C age measurements and by assignment of the well-known ages of Heinrich events (H) 1–6 to our core (Didié et al., 2002).

2.2. Faunal SST reconstructions

Faunal counts were executed in 1 cm steps for the Holocene section and in 2.5 cm steps for the remaining part of the core. A minimum of 300 specimens were counted for each sample. Foraminiferal abundances were examined according to the taxonomic concepts of Saito et al. (1981) and Kennett and Srinivasan (1983).

In total, 29 species were selected for quantitative analyses (Table 1) following in general the strategy of Pflaumann et al. (1996). Intergrades between *Neogloboquadrina pachyderma* dextral (d) and *Neogloboquadrina dutertrei* were grouped together to avoid taxonomic controversies. Left- and right-coiling varieties of *Globorotalia truncatulinoides* were considered separately due to a difference in their temperature preferences (Herman, 1972; Barash, 1988).

To retrieve SSTs from foraminiferal census data alternative statistical approaches of TFT and MAT were applied. The relation between foraminiferal diversities and SSTs was established by using an enlarged Atlantic data base of planktonic foraminiferal counts ('ATL916Lc-epo' http://www.pangaea.de/Institutes/IfG) as well as

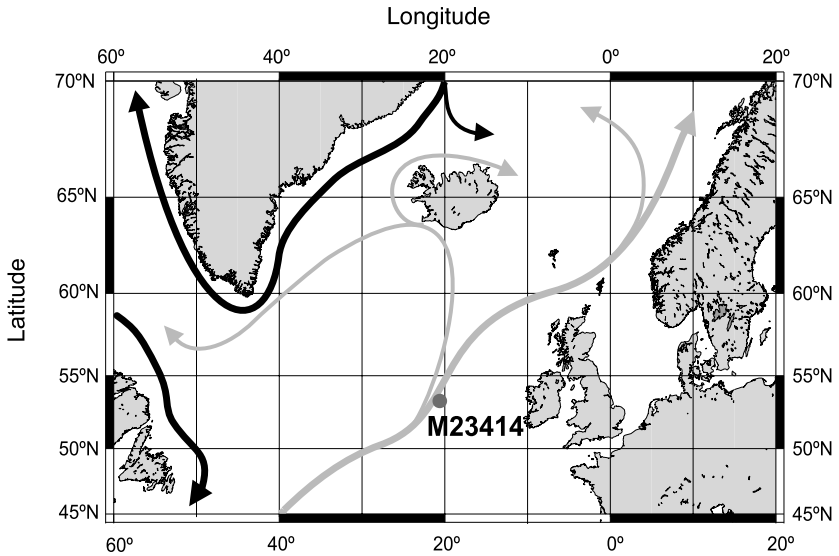

Fig. 1. Generalized surface ocean circulation in the North Atlantic. Geographical position of the investigated core site is indicated. NAD, North Atlantic Drift; gray arrows indicate warm and black arrows cold surface water.

Table 1
Varimax factor score matrix

Species	Factor 1	Factor 2	Factor 3	Factor 4	Factor 5	Factor 6	Factor 7
Globigerinella aequilateralis	−0.002	0.001	0.091	0.008	0.054	−0.021	−0.017
Globigerina bulloides	0.213	0.003	−0.032	**0.937**	0.016	−0.147	−0.148
Globigerina calida	0.005	−0.001	0.015	0.001	0.000	0.018	0.007
Globorotalia conglobatus	−0.002	0.000	0.019	0.000	0.000	0.014	0.000
Globorotalia crassaformis	−0.002	0.001	0.013	−0.003	0.057	0.006	0.002
Sphaeroidinella dehiscens	−0.001	0.000	0.002	−0.002	0.019	0.001	0.003
Beella digitata	0.001	0.000	0.005	0.003	0.015	0.000	−0.004
Neogloboquadrina dutertrei	0.000	0.004	0.022	0.037	**0.628**	0.022	−0.025
Globigerina falconensis	−0.003	−0.002	0.044	0.036	−0.073	0.145	0.034
Globigerinita glutinata	0.142	−0.026	0.142	0.180	−0.057	0.010	**0.493**
Globorotalia hirsuta	−0.007	0.000	0.011	0.043	−0.026	0.057	−0.014
Turborotalita humulis	0.000	−0.001	0.013	0.006	−0.020	0.032	0.000
Globorotalia inflata	0.110	−0.009	0.027	0.107	0.134	**0.930**	−0.003
Candeina nitida	0.000	0.000	0.002	0.000	0.000	−0.001	0.000
Pulleniatina obliquiloculata	−0.003	0.001	0.023	−0.007	0.110	−0.014	0.008
Neogloboquadrina pachyderma (s)	−0.035	**0.993**	−0.003	0.008	−0.012	0.020	−0.077
Neogloboquadrina pachyderma (d)	**0.957**	0.036	0.023	−0.250	−0.006	−0.075	−0.085
Turborotalita quinqueloba	0.047	0.111	−0.011	0.043	0.028	−0.049	**0.841**
Globigerinoides ruber (r)	−0.004	0.002	0.094	−0.008	0.084	−0.056	0.004
Globigerinoides ruber (w)	−0.034	0.005	**0.912**	0.011	−0.225	0.041	−0.054
Globigerina rubescens	0.003	−0.001	0.026	0.013	−0.020	0.011	−0.008
Globigerinoides sacculifer trilobus	−0.016	0.007	0.308	−0.001	0.390	−0.217	−0.068
Globigerinoides sacculifer sacculifer	−0.003	0.002	0.131	−0.030	0.151	−0.077	0.018
Globorotalia scitula	0.018	−0.004	0.011	0.045	−0.011	0.034	0.000
Globigerinoides tenellus	−0.001	0.000	0.025	0.003	−-0.018	0.001	0.002
Globorotalia truncatulinoides (s)	−0.008	0.000	0.039	0.023	−0.056	0.109	0.009
Globorotalia truncatulinoides (d)	0.002	−0.002	0.034	0.044	−0.027	0.083	−0.028
Orbulina universa	0.021	−0.001	0.028	−0.004	0.038	0.026	−0.023
Globorotalia menardii–tumida group	−0.014	0.007	0.084	−0.050	0.565	−0.003	0.063

Bold numbers indicate the dominant species within each factor yielded by PCA.

oceanographic atlas data (Levitus and Boyer, 1994). The census data and factor loadings derived from the TFT procedure were calibrated to the modern seasonal temperatures in the upper 50 m ocean layer. The used winter and summer temperatures represent average values for February–April and August–October, respectively. Because foraminiferal distribution patterns show slightly different temperature responses in the northern and southern hemispheres due to differences in water mass circulation (Barash, 1988; Niebler and Gersonde, 1998), a geographical section of the North Atlantic comprising 721 core top samples was considered for SST estimations.

The TFT factor model was obtained via principal component analysis (PCA) (Imbrie and Kipp, 1971; Klovan and Imbrie, 1971). The resulting total variance of 96% yielded seven factors (Tables 1 and 2). Their geographical distribution resembles in a general way those of earlier factor

Table 2
Statistics of PCA

	Factor 1	Factor 2	Factor 3	Factor 4	Factor 5	Factor 6	Factor 7
Variance	42.30	23.19	16.99	6.02	3.28	2.83	1.39
Cumulative variance	42.30	65.49	82.48	88.50	91.77	94.60	96.00

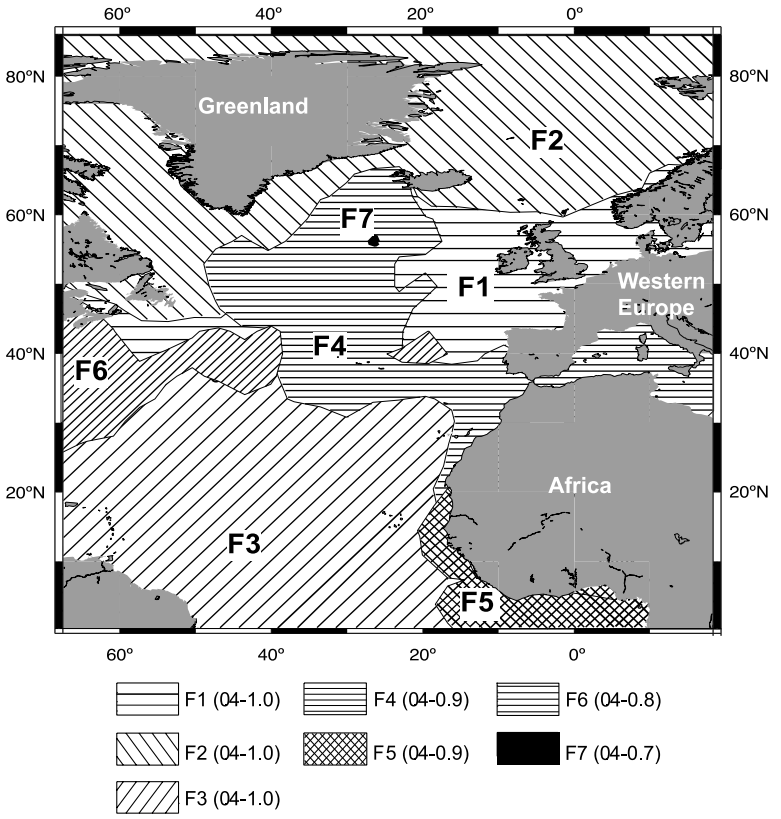

Fig. 2. Generalized geographical distribution of factors resulting from PCA of 721 core tops. Numbers in parentheses show the factor loadings.

models (e.g. Imbrie and Kipp, 1971; Kipp, 1976; Molfino et al., 1982; Hüls and Zahn, 2000), but with the main difference that our model is restricted to the northern hemisphere (Fig. 2). The communalities of the developed factor model are never below 0.7, with a mean value of 0.97. All defined factor loadings were regressed against modern SSTs and the obtained second-degree polynome was then applied to the downcore records (Tables 3 and 4).

A squared chord distance (Overpeck et al., 1985) was chosen to express dissimilarity coefficients (DCs) for MAT. This procedure allows a direct comparison of faunal diversities in a given sample with those of the reference data set. The 10 best analogs were selected for every core sample. All calibration results yield a high statistical robustness for both TFT and MAT (Fig. 3).

The admissible value of DC depends on faunal diversity and has to be determined empirically for every region (Overpeck et al., 1985; Waelbroeck et al., 1998). The DCs within the transitional zone of the North Atlantic, i.e. where our core is located, do not exceed 0.14. For downcore evaluation, this value can therefore be considered as a threshold which allows to distinguish foraminiferal communities adapted to considerably different climate conditions. Excess of this value would mean that the selected best analog samples do not really match with the one analyzed.

2.3. Mg/Ca SST estimation

Mg/Ca measurements have been performed in 5 cm steps to 160 cm (~37.5 ka) and in 10 cm steps for the remaining part of the core. Analyses were executed on temperate-to-subpolar species *Globigerina bulloides* taken from the same sample that

Table 3
Correlation coefficients yielded by TFT regression analysis for winter SST_{0-50m}

	Coefficient	Standard error	Standard coefficient	F to remove
Intercept	12.719	0.557	12.719	521.471
F1	−4.656	0.544	−0.205	73.191
F2	−11.889	0.592	−0.573	403.013
F3	12.555	0.583	0.542	464.037
F5	10.840	1.014	0.239	114.331
F1F2	21.006	2.592	0.280	65.705
F1F4	11.714	1.717	0.212	46.533
F1F5	−13.966	2.459	−0.076	32.254
F1F6	7.483	0.817	0.083	83.914
F1F7	−9.309	1.435	−0.070	42.061
F2F4	−7.968	1.576	−0.049	25.573
F2F7	2.932	0.946	0.025	9.614
F3F4	−8.142	0.789	−0.110	106.379
F3F5	−6.504	1.453	−0.083	20.027
F3F6	−6.527	0.821	−0.71	63.281
F3F7	12.447	2.631	0.034	22.376
F4F5	6.913	2.622	0.031	6.954
F4F7	−15.351	1.552	−0.107	97.821
F1^2	−21.874	5.582	−0.115	15.356
F3^2	−18.540	3.767	−0.122	24.223

have been used for faunal analysis. The cleaning and analysis procedures have been described elsewhere (Müller, 2000; Nürnberg et al., 2000).

The samples were measured on a simultaneous inductively coupled plasma Auger electron spectrometer (ISA Jobin Yion-Spex Instruments S.A. GmbH), selecting undisturbed and most intensive element lines (Mg, 79.55 nm; Ca, 317.93 nm; Y, 371.03 nm as internal standard). Elements were detected by photomultipliers, whose tension was

Table 4
Correlation coefficients yielded by TFT regression analysis for summer SST_{0-50m}

	Coefficient	Standard error	Standard coefficient	F to remove
Intercept	17.578	0.492	17.578	1263.210
F1	−4.469	0.518	−0.206	74.489
F2	−14.685	0.542	−0.741	733.972
F3	8.589	0.525	0.388	267.459
F5	5.870	0.918	0.136	40.877
F1F2	19.151	2.369	0.267	65.372
F1F6	13.060	1.446	0.152	81.607
F1F7	−9.749	1.452	−0.76	45.077
F2F3	31.847	9.995	0.031	10.153
F2F5	−39.897	17.191	−0.032	5.386
F2F7	6.599	1.100	0.060	35.968
F3F4	−3.221	0.702	−0.46	21.036
F3F5	−6.045	1.397	−0.81	18.736
F3f6	−4.581	0.862	−0.052	28.237
F3F7	8.356	2.879	0.024	8.423
F4F7	−14.320	1.576	−0.105	82.558
F5F7	−17.630	6.299	−0.022	7.835
F1^2	−19.085	5.087	−0.105	14.074
F5^2	−15.865	4.391	−0.052	13.051

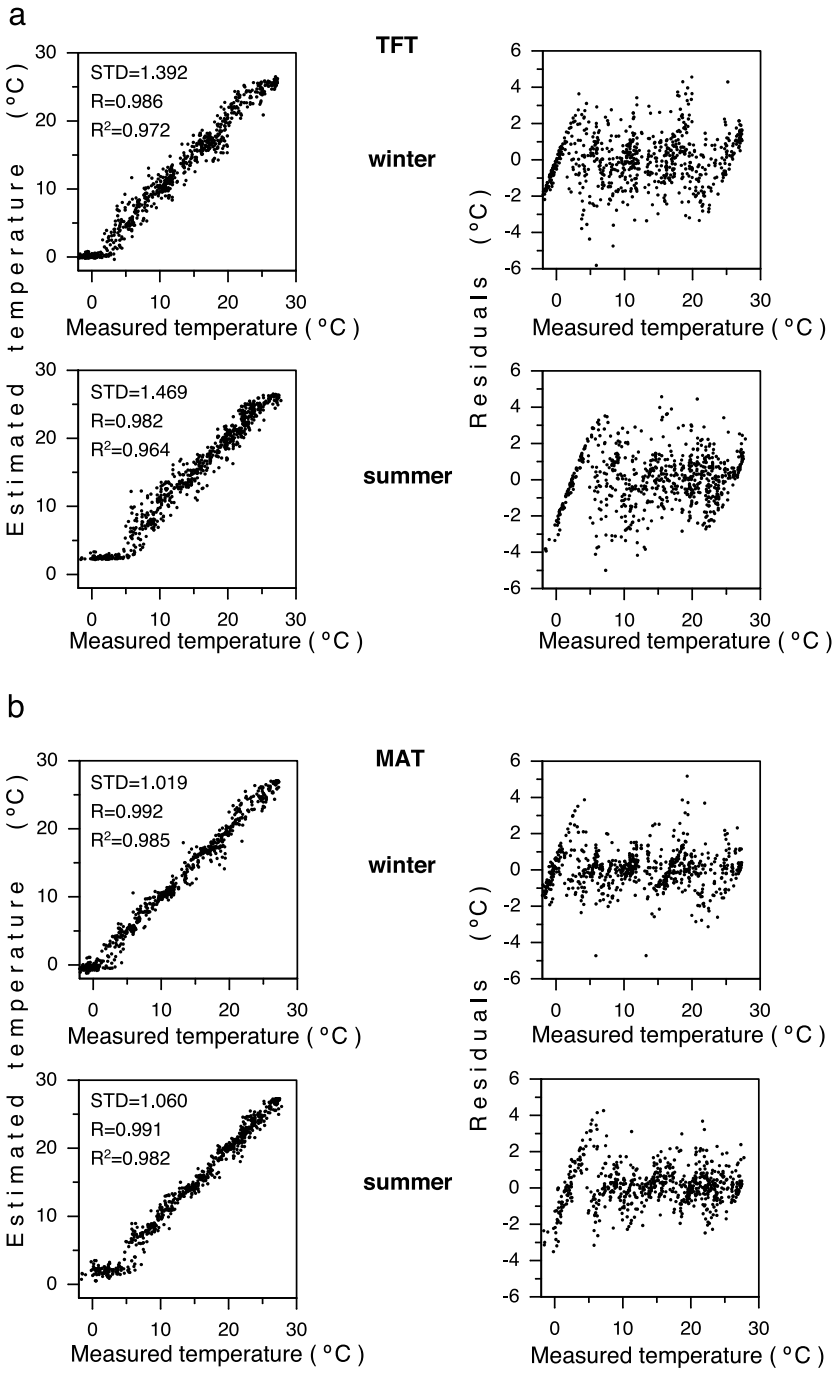

Fig. 3. Measured versus estimated SSTs obtained from the 721 sites of the North Atlantic database for TFT (panel a) and MAT (panel b). *R*, correlation coefficient; STD, standard deviation. SSTs are calculated for the 0–50 m ocean layer.

directly adapted manually for each element concentration. The long-term reproducibility of Mg/Ca is based on 312 analyses of a standard performed over a 3-year period. The standard deviation for the Mg/Ca ratio is 0.124, the standard error is 0.048. The temperatures were calculated using the species-specific calibration curve from Mashiotta et al. (1999).

2.4. Stable oxygen isotope measurements and IRD counts

Stable planktonic isotope records in this study were produced from *Globigerina bulloides* (Jung, 1996; Didié et al., 2002). Measurements were carried out in 2 cm steps back to late MIS 6 and in 5 cm steps for the remaining part of the core. Benthic isotope measurements were carried out on *Cibicidoides wuellerstorfi* in 2.5 cm steps down to the end of MIS 6 and in 5 cm for the remaining part of the core (Jung, 1996).

In order to better interpret the climate changes deduced from the various surface ocean paleodata the IRD record was also considered. These lithic data were originally counted in the >250 μm size fraction and at 2.5 cm depth intervals.

3. Results

3.1. Foraminiferal assemblage changes

Although planktonic foraminiferal assemblages have long been regarded as a sensitive tool for paleoclimatic investigations, as most extant species are adapted to narrow temperature/salinity ranges, more recently published studies rarely analyze changes in multi-species abundance. However, it seems evident that more detailed assemblage analyses down to various species levels should render better paleoSST and interpretation (Chapman et al., 2000; Kandiano and Bauch, 2003). The seven most dominant foraminiferal species in our downcore records comprise 88.8–100% of the total composition (Fig. 4). Changes in relative abundances of these species characterize glacial, interstadial and peak interglacial climate conditions. Relative abundances of the other 15 recognized species never exceed 2%, with a single exception of *Globorotalia truncatulinoides* dextral (d) which reaches up to nearly 6% during MIS 5e.

The polar species *Neogloboquadrina pachyderma* sinistral (s) strongly dominates the glacial core sections, increasing to almost 100% during some 'classical' Heinrich events (e.g. H1, H2, H3 and H11), but also during other pronounced IRD events with the typical Heinrich-like features, such as found during MIS 6 (Fig. 4). In a modern setting *N. pachyderma* (s) comprises 95% of the total assemblage in regions where summer SSTs do not exceed 7°C (Pflaumann et al., 1996) and, therefore, serves as a good marker for polar conditions. In our core this species shows a highly inverse relation with the transitional species *N. pachyderma* (d), the second most dominant species in our record. The latter reaches maxima of 40–45% during peak interglacial conditions. But also warm phases during glacial periods are marked by enhanced relative abundances of *Neogloboquadrina pachyderma* (d). *N. pachyderma* (s) and *N. pachyderma* (d) explain factors 2 and 1, respectively, which have the highest factor loadings (Fig. 5). Therefore, TFT temperature estimates are mainly determined by the interplay between these two factors.

Globigerina bulloides and *Turborotalita quinqueloba* dominate factors 4 and 7, respectively (Fig. 5). These two species tolerate a comparatively wide temperature range. They are, during almost all IRD events, decreasing in abundances but nearly absent during the glacial SST minima of MIS 2 and 6, between 16 and 20 ka and between 142 and 144 ka. *T. quinqueloba* also shows remarkable decreases during peak-interglacial conditions, the Holocene and MIS 5e, because in a modern setting its abundance is greatly reduced in waters warmer than 12°C (Bé and Tolderlund, 1971). Interestingly, abundances of *G. bulloides* and *T. quinqueloba* exhibit clear millennial-scale fluctuations, which are especially pronounced during MIS 3. Their abundances regularly increase immediately before IRD events and experience abrupt decreases coincident with peaks of IRD input.

The cosmopolitan species *Globigerinita glutina-*

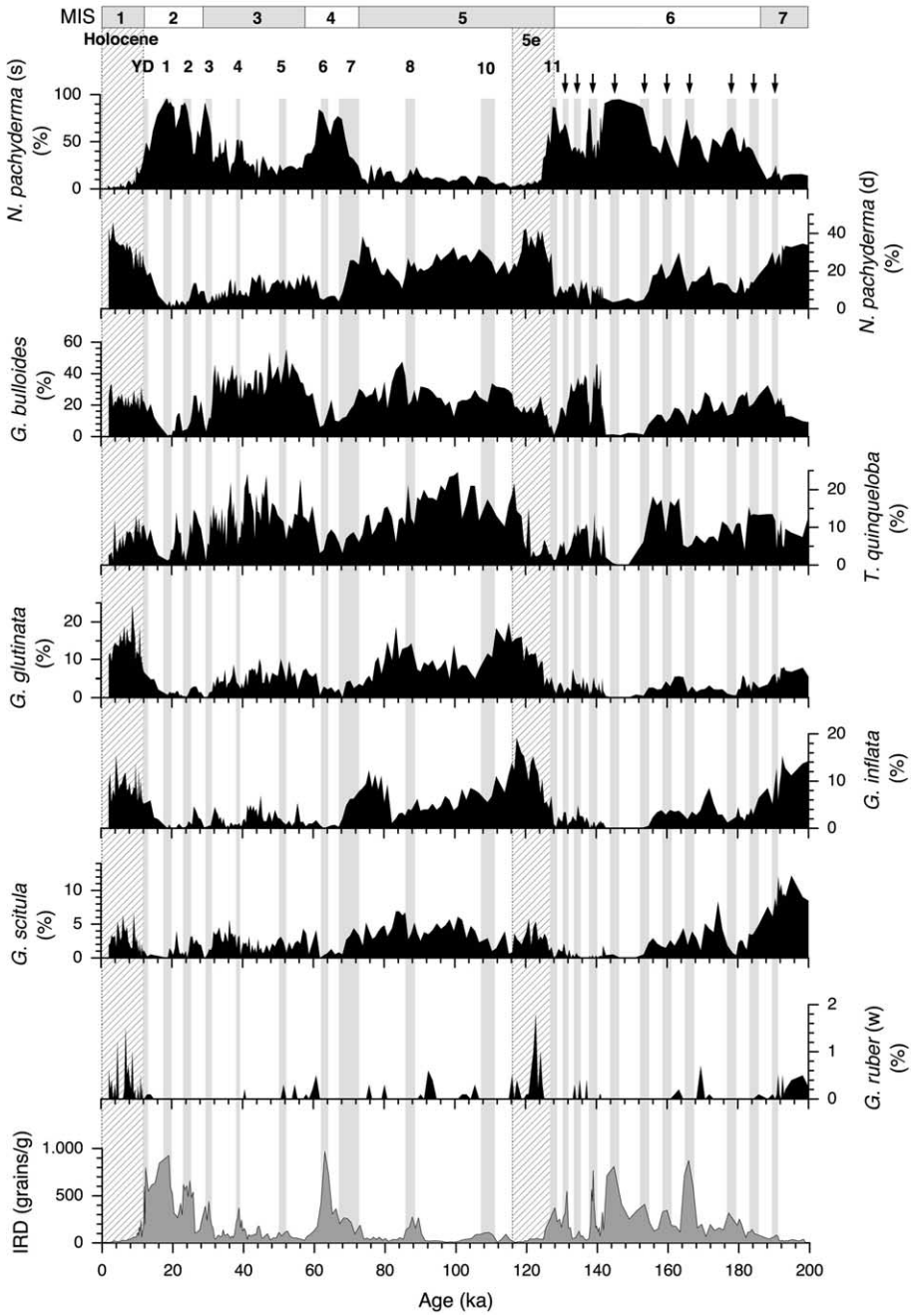

Fig. 4. Records of species distribution and IRD in core M23414 over the last two glacial–interglacial cycles. MIS boundaries are indicated. Numbered gray bars show classical Heinrich events. Arrows indicate Heinrich-like events for MIS 6. Peak interglacial intervals, the Holocene and MIS 5e, are marked by hatched bars. YD, Younger Dryas.

ta and the transitional species *Globorotalia inflata* are more abundant in interglacial core sections, but they also occur during the earlier parts of MIS 6 and MIS 3. Although *G. inflata* is a single contributor to factor 6, its low factor loading along the investigated core (Fig. 5) implies that changes in its abundance do not significantly influence the TFT temperature estimates.

Globorotalia scitula inhabits deeper water masses and occurs in many climatic zones, being adapted to a wide temperature range (Bé and Tolderlund, 1971; Barash, 1988). In our record, this species is strongly reduced only during glacial minima (e.g. MIS 2, 4 and late MIS 6), while in the other core sections, it ranges between 3 and 12% without showing a clear SST preference.

Special consideration must be given to minor members of the foraminiferal assemblage. Although these so-called rare species occur in our records in insignificant amounts, some species

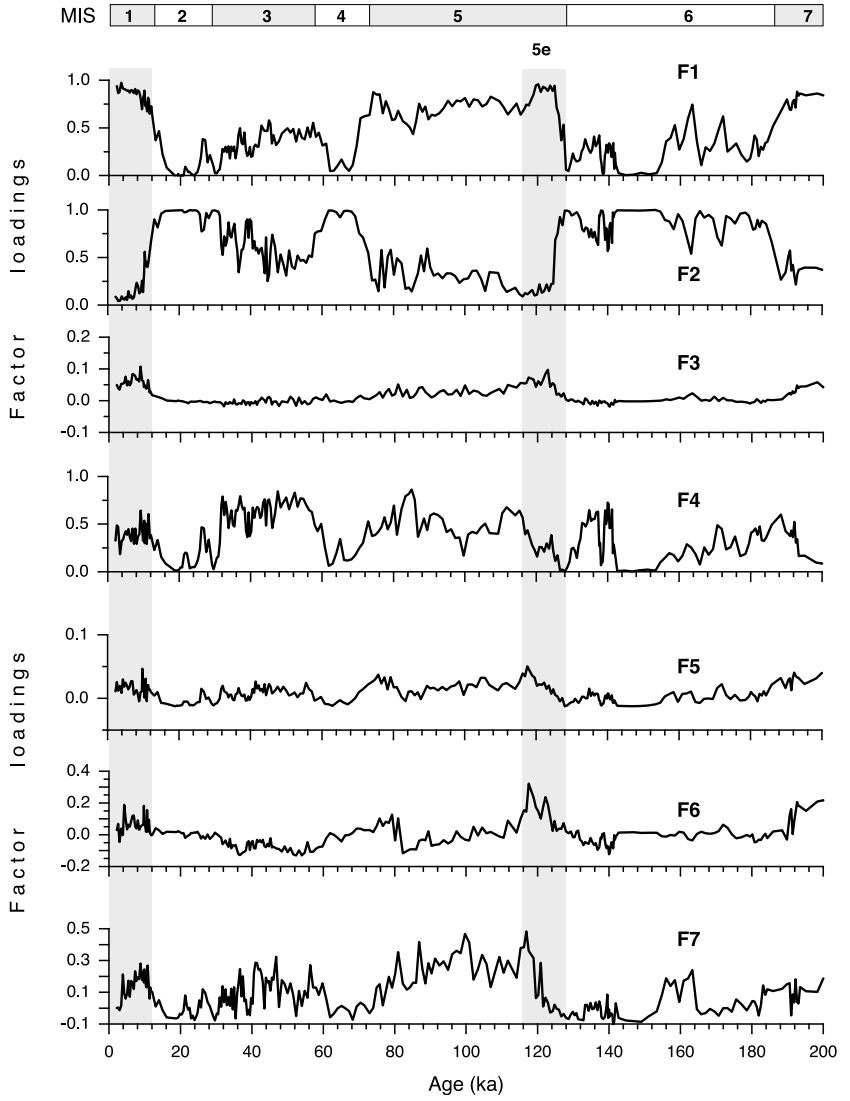

Fig. 5. Distribution of seven factors as yielded by PCA. MIS boundaries are indicated. Peak interglacial intervals, the Holocene and MIS 5e, are marked by hatched bars.

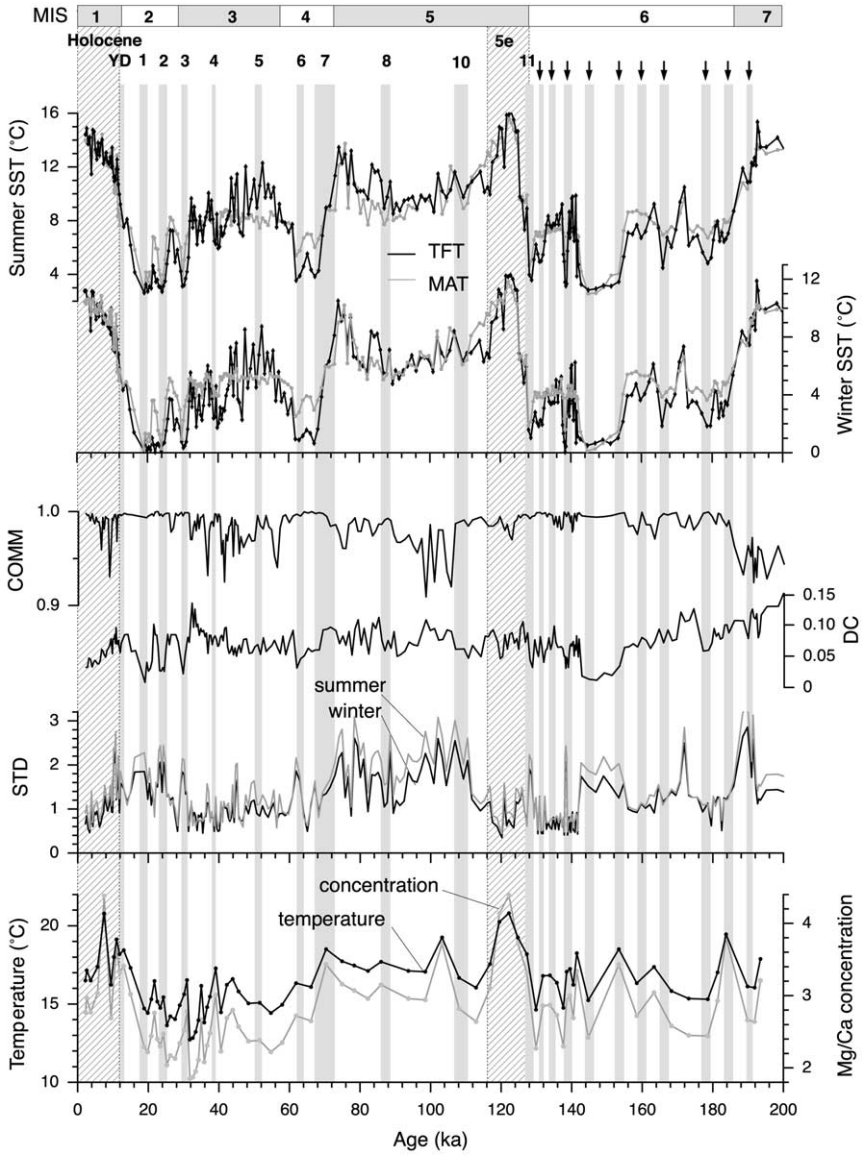

Fig. 6. Comparison of SST estimates based on planktonic foraminiferal diversities (MAT, TFT) and Mg/Ca ratios measured on *Globigerina bulloides*. Faunal SST records are given alongside with communalities (COMM), standard deviations (STD) of selected best analogs, and DCs. Numbered gray bars show classical Heinrich events. Arrows indicate Heinrich-like events for MIS 6. Peak interglacial intervals, the Holocene and MIS 5e, are marked by hatched bars. YD, Younger Dryas.

can be particularly useful in tracing subtle climate differences and/or in indicating some specific paleoceanographic conditions (Bauch, 1994). Intriguingly, a typical tropical dweller, *Globigerinoides ruber* (w), regularly appears within glacial sections, probably indicating short events of warm-water flushes (Fig. 5). Interesting is also that *Globorotalia truncatulinoides* (d) increases its abundance to 6% during MIS 5e whereas in the rest of the core, including the Holocene section, it does not exceed 1%. We have also observed some other tropical species, such as *Globigerinoides conglobatus* and *Hastigerina pelagica*, both during MIS 5e. Although the relative num-

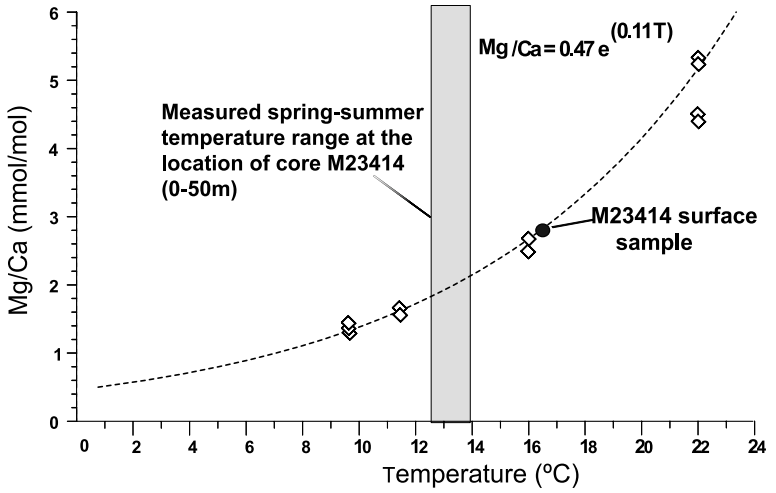

Fig. 7. Mg/Ca-temperature calibration curve derived from culturing experiments of *Globigerina bulloides* (Mashiotta et al., 1999). Summer SST calculated from M23414 core top sample and average spring–summer SST measured at site M23414 (Levitus and Boyer, 1994) are indicated.

ber of these tropical species is negligible, their sole occurrence may imply some differences in the ecological and/or paleoceanographical situation during MIS 5e in comparison to the Holocene.

3.2. Faunal SSTs, $\delta^{18}O$ and IRD records

Calculated core-top SSTs of 10.4 and 14.0°C (MAT) and 11.2 and 14.4°C (TFT) for winter and summer, respectively, agree well with modern observations (winter = 10.6°C; summer = 13.8°C; Levitus and Boyer, 1994). Over the entire investigated time interval, both sets of paleoSST estimates reveal a good correspondence (Fig. 6) by showing the same general trends within the combined error of each method (2.4°C for winter and 2.5°C for summer).

The communalities and dissimilarity indices, which control the consistency of the obtained results for TFT and MAT respectively, are within an acceptable range (Fig. 6), with the exception of parts of MIS 7 when DCs exceed the admissible value. The registered communality minimum within the investigated interval is 0.91 and the mean is 0.99. This clearly shows that all examined samples match well with the obtained model.

Standard deviations of the best analogs selected by the MAT procedure range from 0.4 to 3.3°C (Fig. 6). Increased standard deviation values are not coincident with increased DCs. For instance, the temperature minimum observed during MIS 6, between 144 and 156 ka, is characterized by lowest DCs but enhanced standard deviations which are related to the 'cold-end' temperature problem, when the summer temperature ranges between −1.6 and 7°C with a dominance of up to 95% of *Neogloboquadrina pachyderma* (s) (Pflaumann et al., 1996).

An SST offset of up to 2.5°C between MAT and TFT results is obtained between 56 and 68 ka and for the time 85 ka, 116 ka. This discrepancy can be explained by the fact that our TFT estimates are mostly driven by the interplay between polar and temperate factors, which both exhibit the highest factor loadings in our records. These two factors are in turn mainly determined by the distribution of *Neogloboquadrina pachyderma* (s) and *N. pachyderma* (d), respectively (Fig. 5). Other species have very low scores (Tables 1 and 3) in these factors, and changes in abundances of predominant species are translated into temperature calculations with some overriding. Thus, when applying MAT and TFT together we obtain a better control on the generated temperature estimates.

SSTs reach their maxima during peak intergla-

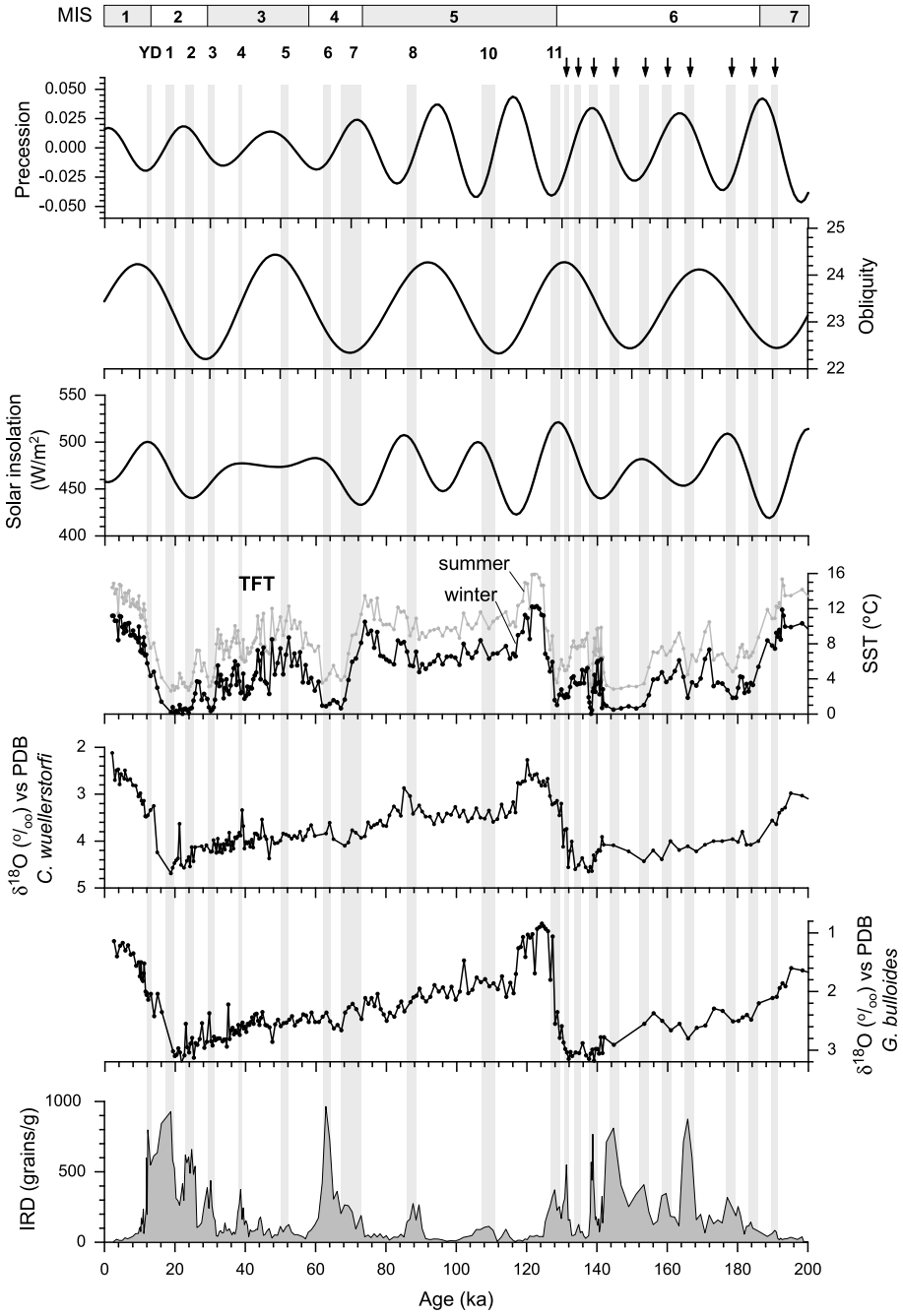

Fig. 8. Comparison of downcore records (faunal SSTs derived from TFT; planktonic and benthic oxygen isotope; IRD) with Earth obliquity and precession and early June solar insolation calculated for 65°N (Berger, 1978). Heinrich and Heinrich-like events are indicated in gray bars. Numbered gray bars show classical Heinrich events. Arrows indicate Heinrich-like events for MIS 6. Vertical lines represent MIS boundaries. YD, Younger Dryas.

cial conditions. In MIS 5e, temperatures are 16 and 12°C for summer and winter, respectively (Fig. 6), which is ~2°C higher than during the Holocene. Glacial temperatures are in general 8–9°C colder than peak interglacial ones. They reach their minima of 0 and 3.5°C for winter and summer, respectively, during the late MIS 6 (around 138 ka and between 144 and 156 ka) and during MIS 2 (between 20 and 24 ka). The TFT estimates yield another temperature minimum in MIS 4 (between 56 and 66 ka), which is also reflected in a remarkable decrease of *Neogloboquadrina pachyderma* (d).

Contrary to MAT, millennial-scale variability is more pronounced in the TFT temperature record, which shows larger amplitude. The amplitude ranges between 3 and 6°C during glacial periods but notably less during interglacial and, especially, during peak-interglacial time intervals. The most pronounced abrupt temperature decreases are coincident with IRD events (Fig. 6). These repeatedly punctuate the colder time intervals.

On the glacial–interglacial time scale, the planktonic $\delta^{18}O$ record derived from *Globigerina bulloides* is in general agreement with both sets of SST estimates based on foraminiferal diversity (Fig. 8). The lighter isotope excursion found during the peak of MIS 5e in comparison to the Holocene supports the results of the census data. During each glacial evolution the planktonic $\delta^{18}O$ record shows a gradual increase that culminates before the terminations. Interestingly, the SST minimum during the last glaciation is coincident with heaviest planktonic as well as benthic $\delta^{18}O$ values whereas during the penultimate glaciation the SST minimum clearly precedes the maximum in both $\delta^{18}O$ records. The millennial-scale variability is not well expressed in planktonic isotope records of *G. bulloides*. In most cases it reflects neither initial cooling, which is a characteristic feature of abrupt climate changes in the North Atlantic, nor enhanced input of freshwater from melting icebergs.

3.3. Mg/Ca thermometry

The Mg/Ca ratios measured on *Globigerina bulloides* exhibit a relatively clear temperature-dependent trend (Fig. 6). The Mg/Ca ratios show values between 1.9 and 4.4 mmol/mol. The glacial Mg/Ca ratios vary between 1.9 and 3.8 mmol/mol with the lowest values noted during late MIS 3. Interglacial peaks are marked by maxima in Mg/Ca ratio that increase up to 4.4 mmol/mol. Although the spatial sample resolution of our Mg/Ca analyses is not sufficient to trace millennial-scale variability in detail, major IRD events are still recognizable by a decrease in Mg/Ca ratios of up to 1 mmol/mol.

Because *Globigerina bulloides* undergoes growth and reproductive stages between 0 and 60 m water depth in the mid-latitudes of the eastern North Atlantic during April to June (Ottens, 1992; Schiebel et al., 1997), it can be assumed that temperatures derived from Mg/Ca reflect the spring-to-summer SST values of the upper 60 m ocean layer. Thus, our calculated temperatures of 20.8°C during peak-interglacial conditions and the minimum of 13°C during late MIS 3 seem to be an overestimation. This gains support from the calculated estimate of 16.5°C for the core-top sample, a value which already exceeds the SST of the 50 m layer depth in May by 4.4°C (Fig. 7; Levitus and Boyer, 1994).

4. Discussion

The faunal SST records derived from two alternative techniques together with analysis of the species composition of planktonic foraminifera enable us to decipher in more detail the climate dynamics over the last two glacial–interglacial cycles. In addition, availability of well proven faunal SST estimates makes it possible to evaluate the applicability of Mg/Ca-derived temperatures in a climatically important area of the Northeast Atlantic.

4.1. Comparison of major glacial–interglacial trends

A comparison of these two intervals reveals some differences in their climate evolution in the North Atlantic. Contrary to the last glacial cycle

when the glacial maximum immediately preceded Termination I, during MIS 6 the long-lasting glacial SST minimum between 144 and 156 ka occurred well before the final onset of Termination II, approximately 9 kyr according to the ice-volume-based SPECMAP chronology (Martinson et al., 1987; Figs. 6 and 8). A similar time discrepancy for the glacial termination of MIS 6 has been suggested previously by Winograd et al. (1992) and it could well be that during the course of MIS 6, the development of ice-sheet growth and temperatures on the subpolar northern hemisphere was not synchronous. This is supported by a recent comparison of ice-core data with benthic $\delta^{18}O$ which led to the assumption that the phase lag between temperature dynamics and ice-volume response is a general feature of the late Pleistocene climate system (Shackleton, 2000).

Because the temperature minimum between 144 and 156 ka was associated with enhanced IRD input and a dominance of *Neogloboquadrina pachyderma* (s) (Figs. 4 and 6) it is evident that site 23414 was already occupied by polar water masses. Interesting in this respect is that a corresponding cold minimum during the middle of MIS 6 is not registered by SST estimates further south, at 43°N and at 48°N (Madureira et al., 1997; Calvo et al., 2001). This difference in latitudinal SST would place the polar front somewhere between 48° and 53°N and, moreover, it would imply the existence of a rather steep meridional temperature gradient between our location and the region further south. Most likely, the position of the polar front prevented the propagation of warm surface waters northward. This can be inferred from the nearly complete absence of foraminiferal species other than *N. pachyderma* (s) during the SST minimum between 144 and 156 ka. The general pattern of surface water circulation could have been similar to that reconstructed for the last glacial maximum, when ocean heat was stored within a clockwise gyre to the south of the polar front (Chapman and Maslin, 1999). The appearance of such a long-lasting temperature minimum in the middle of the previous glaciation could be explained by specific dynamics of changes in the orbital parameters characteristic for MIS 6. Contrary to the relatively short insolation minimum at the end of MIS 2, when obliquity and precession forcing were in-phase, these two orbital parameters were out of phase during MIS 6 (Fig. 8).

Supported by the appearance of rare tropical species our faunal SSTs as well as the planktonic $\delta^{18}O$ record indicate a warmer character of MIS 5e compared to the Holocene (Figs. 6 and 8). The 2°C difference between MIS 5e and 1 on the basis of our faunal SSTs is about the same as that inferred from pollen records for a similar latitude in France (e.g. Guiot et al., 1993), corroborating the overall strong connection between western European climate conditions and the particular state of the THC in the Northeast Atlantic (Kukla et al., 1997).

4.2. Climate changes on short time scales

Millennial-scale SST variability is strongly expressed in the faunal data during both the colder glacial periods and the more temperate intervals of MIS 5a–d. Our records show that the typical nature of Heinrich events, as investigated in detail for the last 130 ka (e.g. Bond et al., 1993; McManus et al., 1994; Bond and Lotti, 1995; Oppo and Lehmann, 1995; Sarnthein et al., 2001), also existed during the penultimate glaciation despite the difference found between the major glacial trend and orbital forcing. Indeed, during both glacial cycles the characters of abrupt climate events show identical regularities. The slight decreases in SSTs registered immediately prior to a major abrupt climate cooling event with enhanced IRD (Bond and Lotti, 1995; van Kreveld et al., 2000) imply that the Laurentide–Greenland ice sheet, which is considered to be the main contributor of IRD delivery to the North Atlantic (e.g. Gwiazda et al., 1996), responded rapidly to initial climate cooling. Although our records do not directly show the characteristic SST decreases, the short climate cooling episodes can be recognized by some distinct faunal changes: every major increase in *Neogloboquadrina pachyderma* (s) abundance is often led by excursions of *Globigerina bulloides* and *Turborotalita quinqueloba*, species that are able to tolerate temperature decreases down to 1°C (Bé and Tolderlund, 1971) and con-

stitute, along with *N. pachyderma* (s), considerable parts of the modern assemblage in the subarctic region (Johannessen et al., 1994; Bauch, 1997; Carstens et al., 1997). Similar increases in abundance of *G. bulloides* prior to Heinrich events were also reported from further south of our location (Chapman et al., 2000). It altogether underlines the need to also consider other faunal information than that provided by the relative abundance of *N. pachyderma* (s) and SSTs alone. This is because both latter proxy methods consider one or a few dominant species, which may suppress the importance of less abundant species, eventually leading to a certain loss of some relevant paleoceanographic information.

Paleoclimatic records and modeling experiments show that meltwater delivered from icebergs distorts THC (Oppo and Lehmann, 1995; Seidov and Maslin, 1999; Ganopolski and Rahmstorf, 2001), thus causing further cooling. Since such a situation persists until freshwater input decreases and THC is reinitiated, the occurrence of the tropical species *Globigerinoides ruber* may be taken as evidence of these initial flushes of warm water. We may further assume that some modulations of the THC characterize Dansgaard–Oeschger events, because *G. ruber* repeatedly occurred in between Heinrich events. At present, however, more studies on this rare species are required from this part of the North Atlantic in order to further substantiate such an interpretation.

4.3. *Assessment of climate proxies in* Globigerina bulloides

Because *Globigerina bulloides* can tolerate a comparatively large temperature range, this species occurs in considerable abundances in various climate zones and is therefore often used for paleoceanographic investigations. Our direct comparison of chemical proxies and faunal SSTs, however, indicates some difficulties when employing *G. bulloides*. Despite good calibration of Mg/Ca ratios and temperatures obtained from cultural experiments (Mashiotta et al., 1999), paleoSSTs at our location calculated using this equation seem to be largely overestimated. The difference between faunal and Mg/Ca-derived temperatures reaches as much as 10–13°C. Such a discrepancy casts doubts on using changes in Mg concentration of *G. bulloides* tests in the Northeast Atlantic as a proxy for temperatures. Nevertheless, the major glacial–interglacial trend expressed in the chemical record implies existence of a temperature-dependent signal. The large offsets noted between Mg/Ca and faunal-derived SSTs may partly be accounted for by the fact that the cultural experiments did not include the temperature range below 10°C. But this cannot explain the large deviations of the obtained results for peak interglacial intervals, when SSTs were well above 10°C; this general picture does not change either when using the new calibration by Elderfield and Ganssen (2000) based on cultural experiments and core tops, which also takes into account a lower temperature range. Moreover, compared to Mg/Ca temperatures derived from other species, those from *G. bulloides* show the largest scatter (Elderfield and Ganssen, 2000).

It is therefore also likely that, along with temperature changes, additional factors control the Mg uptake in *Globigerina bulloides*. On the basis of cultural experiments it was found that salinity changes of the ambient sea water do have an influence on the Mg concentrations (Nürnberg et al., 1996). In comparison to temperature changes, however, those of salinity cause only a minor effect in Mg uptake. Moreover, because the Mg/Ca ratio in foraminiferal tests decreases with salinity reduction, meltwater overprints which typically occurred during IRD events could cause an underestimation of the Mg/Ca-derived temperature. But in the glacial section of the investigated core the excess of Mg/Ca temperatures over those derived from faunal census counts is much higher (10°C in average) than for the peak interglaciations (~4°C). Another possible explanation comes from genetic evidence, which indicates that the species concept of *G. bulloides* is complicated by the existence of different genotypes (Darling et al., 2000) with a different water mass relation (Stewart et al., 2001). Thus, experimental laboratory calibration produced by Mashiotta et al. (1999) may well suit certain regions (e.g. Pahnke et al., 2003), but may not necessarily be

applicable for the specific conditions of the Northeast Atlantic.

In our record and in others from the region (e.g. Venz et al., 1999), also oxygen isotope data derived from *Globigerina bulloides* show some limitations. Although the major glacial–interglacial trends are clearly recognizable, isotopic substages as well as short-term climate changes are not well pronounced. It has been shown that temperature signals in oxygen isotope records of certain species are well expressed only within a temperature range which provides optimal conditions for this species (Mix, 1987; Bäckström et al., 2001). It could well be that during major IRD events SSTs were at the lower limit or even dropped beyond the temperature range characteristic for *G. bulloides*. Such a situation could have caused a shift of its major reproductive cycle into a different, warmer season of the year. Due to such seasonal shifts the influence of temperature on the oxygen isotope signature becomes more pronounced (Mix, 1987). Particularly for the Northeast Atlantic it can be assumed that the enhanced iceberg melting that occurred repeatedly during times other than peak interglacials caused strong stratification of the upper ocean layer. Such a situation affected both the thermocline thickness and the depth of the pycnocline (e.g. Labeyrie et al., 1995), which would further complicate the interpretation of both the Mg/Ca ratio and $\delta^{18}O$ proxy in terms of SST changes.

5. Conclusive summary

Multiproxy paleoceanographic records have been obtained from a sediment core underlying the NAD in order to examine the glacial–interglacial as well as millennial-scale climate fluctuations during 200 ka. Paleotemperature estimates, derived from foraminiferal census data, were calculated using the methods of TFT and MAT. Faunal SSTs were compared to SST results calculated from Mg/Ca in *Globigerina bulloides* and are supported by benthic and planktonic isotope data and IRD records.

Both faunal SST sets show high coincidence in absolute values. Supported by the appearance of tropical species, MIS 5e appears to be as much as 2°C warmer than the Holocene on the basis of faunal SST records. The evolution of the last two glacial periods reveals some differences. In contrast to the last glaciation, when the temperature minimum occurred roughly time-coeval with the minimum in solar irradiance immediately preceding Termination I, during the penultimate glaciation the most prolonged and severe cold interval appeared when insolation was at an intermediate level, between 156 and 144 ka. This discrepancy in glacial development was most likely caused by differences in the orbital configuration.

Millennial-scale climate oscillations during colder times reveal the same order of principal steps along the entire investigated interval, implying a strong systematic nature of climate forcing factors and their effects on the environmental system. Each event started with a slight positive response in the abundance of subpolar species. The next step is marked by an IRD event coincident with a considerable decrease in SST of up to 3–5°C and eventually terminates in an abrupt warming which brings the system back to its initial state.

In order to assess the applicability of Mg/Ca thermometry performed on *Globigerina bulloides*, temperature estimates derived from this method were compared with faunal SSTs. The comparison revealed a considerable offset between the results, implying that Mg/Ca temperatures are largely overestimated; however, they follow the general glacial–interglacial trend in the Northeast Atlantic and, therefore, have the potential to yield paleoceanographic information for this climatically important region. The large overestimation of Mg/Ca-derived SST results may be explained by involvement of other factors that influence the Mg uptake in *G. bulloides* tests and/or by the existence of different genotypes of this species with a different water mass relation. Also, seasonal shifts in bioproductivity, which may be inferred for time intervals near the lower temperature tolerance of *G. bulloides*, can cause further complications when interpreting the final results. For the same reasons it may also help to explain the fact that the isotope record of *G. bulloides* clearly expresses the

general glacial–interglacial trends but is muted in its amplitude when it comes to shorter-term climate changes. Thus, in order to better assess its climatic potential there seems to be a need to further explore the relation of *G. bulloides* in terms of its habitat under different oceanographic settings.

Acknowledgements

The manuscript benefited from suggestions and comments made by two reviewers, W.F. Ruddiman and anonymous. The study was financially supported through grants from 'Deutsche Forschungsgemeinschaft' (Schm250/4; Du129/33-1; Th200/40-1).

References

Bäckström, D.L., Kuijpers, A., Heinemeier, J., 2001. Late Quaternary North Atlantic paleoceanographic records and stable isotopic variability in four planktonic foraminiferal species. J. Foraminifer. Res. 31, 25–31.

Barash, M.S., 1988. Chetvertichnaya palaeoceanologya Atlanticheskogo oceana. Nauka, Moscow (in Russian).

Bauch, H., 1994. *Beella megastoma* (Earland) in late Pleistocene Norwegian-Greenland sea sediments: stratigraphy and meltwater implication. J. Foraminifer. Res. 24, 171–177.

Bauch, H.A., 1997. Paleoceanography of the North Atlantic Ocean (68°-76°N) during the past 450 ky deduced from planktic foraminiferal assemblages and stable isotopes. In: Hass, H.C., Kaminski, M.A. (Eds.), Contributions to the Micropaleontology and Paleoceanography of the Northern North Atlantic. Grzybowski Foundation Spec. Publ., Krakow, pp. 83–100.

Bé, A.W.H., Tolderlund, D.S., 1971. Distribution and ecology of living planktonic foraminifera in surface waters of the Atlantic and Indian oceans. In: Funnel, B.M., Riedel, W.R. (Eds.), The Micropaleontology of the Oceans. Cambridge University Press, Cambridge, pp. 105–149.

Berger, A., 1978. Long-term variations of daily insolation and Quaternary climatic change. J. Atmos. Sci. 35, 2362–2367.

Bond, G.C., Lotti, R., 1995. Iceberg discharges into the North Atlantic on millennial time scales during last glaciation. Science 267, 1005–1010.

Bond, G., Heinrich, H., Broecker, W., Labeyrie, L., McManus, J., Andrews, J., Huon, S., Jantschik, R., Clasen, S., Simet, C., Tedesco, K., Klas, M., Bonani, G., Ivy, S., 1992. Evidence for massive discharge of icebergs into the North Atlantic ocean during the last glacial period. Nature 360, 245–249.

Bond, G., Broecker, W., Johnsen, S., McManus, J., Labeyrie, L., Jouzel, J., Bonani, G., 1993. Correlations between climate records from North Atlantic sediments and Greenland ice. Nature 365, 143–147.

Broecker, W.S., Denton, G.H., 1990. The role of ocean-atmosphere reorganizations in glacial cycles. Quat. Sci. Rev. 9, 305–341.

Calvo, E., Villanueva, J., Grimalt, J.O., Boelaert, A., Labeyrie, L., 2001. New insights into the glacial latitudinal temperature gradients in the North Atlantic. Results from $U^{K'}_{37}$ sea surface temperatures and terrigenous inputs. Earth Planet. Sci. Lett. 188, 509–519.

Carstens, J., Hebbeln, D., Wefer, G., 1997. Distribution of planktic foraminifera at the ice margin in the Arctic (Fram Strait). Mar. Micropaleontol. 29, 257–269.

Chapman, M.R., Maslin, M.A., 1999. Low-latitude forcing of meridional temperature and salinity gradients in the subpolar North Atlantic and the growth of glacial ice sheets. Geology 27, 875–878.

Chapman, M.R., Shackleton, N.J., Duplessy, J.-C., 2000. Sea surface temperature variability during the last glacial-interglacial cycle: assessing the magnitude and pattern of climate change in the North Atlantic. Palaeogeogr. Palaeoclimatol. Palaeoecol. 157, 1–25.

Clark, P.U., Pisias, N.G., Stocker, T.F., Weaver, A.J., 2002. The role of the thermohaline circulation in abrupt climate change. Nature 415, 863–869.

Dansgaard, W., Johnsen, S.J., Clausen, H.B., Dahl-Jensen, D., Gundestrup, N.S., Hammer, C.U., Hvidberg, C.S., Steffensen, J.P., Sveinbjörnsdottir, A.E., Jouzel, J., Bond, G., 1993. Evidence for general instability of past climate from a 250-kyr ice-core record. Nature 364, 218–220.

Darling, K.F., Wade, C.M., Stewart, I.A., Kroon, D., Dingle, R., Brown, A.J.L., 2000. Molecular evidence for genetic mixing of Arctic and Antarctic planktonic foraminifers. Nature 405, 43–47.

Didié, C., Bauch, H.A., 2000. Species composition and glacial-interglacial variations in the ostracode fauna of the northeast Atlantic during the past 200,000 years. Mar. Micropaleontol. 40, 105–129.

Didié, C., Bauch, H.A., Helmke, J.P., 2002. Late Quaternary deep-sea ostracodes in the polar and subpolar North Atlantic: paleoecological and paleoenvironmental implications. Palaeogeogr. Palaeoclimatol. Palaeoecol. 184, 195–212.

Duplessy, J.-C., Shackleton, N.J., Fairbanks, R., Labeyrie, L., Oppo, D., Kallel, N., 1988. Deepwater source variations during the last climatic cycle and their impact on the global deepwater circulation. Paleoceanography 3, 343–360.

Elderfield, H., Ganssen, G., 2000. Past temperature and $\delta^{18}O$ of surface ocean waters inferred from foraminiferal Mg/Ca ratios. Nature 405, 442–445.

Ganopolski, A., Rahmstorf, S., 2001. Rapid changes of glacial climate simulated in a coupled climate model. Nature 409, 153–158.

Grootes, P.M., Stuiver, M., 1997. Oxygen 18/16 variability in Greenland snow and ice with 10^{-3} to 10^{-5}-year time resolution. J. Geophys. Res. 102, 26455–26470.

Grootes, P.M., Stuiver, M., White, J.W.C., Johnsen, S., Jouzel, J., 1993. Comparison of the oxygen isotope records from the GISP 2 and GRIP Greenland ice cores. Nature 366, 552–554.

Grousset, F.E., Labeyrie, L., Sinko, J.A., Cremer, M., Bond, G., Duprat, J., Cortijo, E., Huon, S., 1993. Patterns of ice-rafted detritus in the glacial North Atlantic (40°-55°N). Paleoceanography 8, 175–192.

Guiot, J., de Beaulieu, J.L., Cheddadi, R., David, F., Ponel, P., Reille, M., 1993. The climate in Western Europe during the last Glacial/Interglacial cycle derived from pollen and insect remains. Palaeogeogr. Palaeoclimatol. Palaeoecol. 103, 79–93.

Gwiazda, R.H., Hemming, S.R., Broecker, W.S., 1996. Provenance of icebergs during Heinrich event 3 and the contrast to their sources during other Heinrich events. Paleoceanography 11, 371–378.

Heinrich, H., 1988. Origin and consequences of cyclic ice-rafting in the northeast Atlantic Ocean during the past 130,000 years. Quat. Res. 29, 142–152.

Helmke, J.P., Bauch, H.A., 2001. Glacial-interglacial relationship between carbonate components and sediment reflectance in the North Atlantic. Geo-Mar. Lett. 21, 16–22.

Helmke, J.P., Schulz, M., Bauch, H.A., 2002. Sediment color record reveals patterns of millennial-scale climate variability over the last 500,000 years. Quat. Res. 57, 16–22.

Herman, Y., 1972. *Globorotalia truncatulinoides*: a Palaeoceanographic indicator. Nature 238, 394–396.

Hüls, M., Zahn, R., 2000. Millennial-scale sea surface temperature variability in the western tropical North Atlantic from planktonic foraminiferal census counts. Paleoceanography 15, 659–678.

Imbrie, J., Kipp, N.G., 1971. A new micropaleontological method for quantitative paleoclimatology: Application to a Late Pleistocene Caribbean core. In: Turekian, K.K. (Ed.), The Late Cenozoic Glacial Ages. Yale University Press, New Haven, pp. 71–181.

Johannessen, T., Jansen, E., Flatoy, A., Ravelo, A.C., 1994. The relationship between surface water masses, oceanographic fronts and paleoclimatic proxies in surface sediments of the Greenland, Iceland, Norwegian Seas. In: Zahn, R., Pedersen, T.F., Kaminski, M.A., Labeyrie, L. (Eds.), Carbon Cycling in the Glacial Ocean: Constraints of the Oceans's Role in Global Change. Springer, Berlin, pp. 61–85.

Johnsen, S.J., Clausen, H.B., Dansgaard, W., Fuhrer, K., Gundestrup, N., Hammer, C.U., Iversen, P., Jouzel, J., Stauffer, B., Steffensen, J.P., 1992. Irregular glacial interstadials recorded in a new Greenland ice core. Nature 359, 311–313.

Jung, S.J.A., 1996. Wassermassenaustausch zwischen NE-Atlantik und Nordmeer während der letzten 300.000/80.000 Jahre im Abbild stabiler O- und C-Isotope. Berichte Sonderforschungber. 313 (61), Christian-Albrechts University, Kiel (in German).

Kandiano, E.S., Bauch, H.A., 2003. Surface ocean properties in the Northeast Atlantic during the last 500,000 years: Evidence from foraminiferal census data and iceberg-rafted debris. Terra Nova 15, 265–271.

Kennett, J.P., Srinivasan, M.S., 1983. Neogene Planktonic Foraminifera - A Phylogenetic Atlas. Hutchinson Ross, Stroudsburg, PA.

Kipp, N., 1976. New transfer function for estimating past sea surface conditions from sea bed distribution of planktonic foraminiferal assemblages in the North Atlantic. In: Cline, R.M., Hays, J.D. (Eds.), Investigation of Late Quaternary Paleoceanography and Paleoclimatology. Geol. Soc. Am. Mem., pp. 3–41.

Klovan, J.E., Imbrie, J., 1971. An algorithm and fortran IV program for large-scale Q-Mode factor analysis and calculation of factor scores. Math. Geol. 3, 61–77.

Kukla, G., McManus, J.F., Rousseau, D.-D., Chuine, I., 1997. How long and how stable was the last interglacial? Quat. Sci. Rev. 16, 605–612.

Labeyrie, L., Vidal, L., Cortijo, E., Paterne, M., Arnold, M., Duplessy, J., Vautravers, M., Labracherie, M., Duprat, J., Turon, J., Grousset, F., Van Weering, T., 1995. Surface and deep hydrology of the northern Atlantic ocean during the past 150000 years. Philos. Trans. R. Soc. London B 348, 255–264.

Levitus, S., Boyer, T.P., 1994. World Ocean Atlas 1994: Temperature. U.S. Department of Commerce, Washington, DC.

Madureira, L.A.S., van Kreveld, S., Eglinton, G., Conte, M.H., Ganssen, G., van Hinte, J.E., Ottens, J.J., 1997. Late Quaternary high-resolution biomarker and other sedimentary climate proxies in a northeast Atlantic core. Paleoceanography 12, 255–269.

Marotzke, J., 2000. Abrupt climate change and thermohaline circulation: Mechanisms and predictability. Proc. Natl. Acad. Sci. 97, 1347–1350.

Martinson, D.G., Pisias, N.G., Hays, J.D., Imbrie, J., Moore, T.C., Shackleton, N.J., 1987. Age dating and the orbital theory of the Ice Ages: Development of a high-resolution 0 to 300,000-year chronostratigraphy. Quat. Res. 27, 1–29.

Mashiotta, A.T., Lea, D.W., Spero, H.J., 1999. Glacial-interglacial changes in Subantarctic sea surface temperature and δ^{18}O-water using foraminiferal Mg. Earth Planet. Sci. Lett. 170, 417–432.

McManus, J.F., Bond, G.C., Broecker, W.S., Johnsen, S., Labeyrie, L., Higgins, S., 1994. High-resolution climate records from the North Atlantic during the last interglacial. Nature 371, 326–329.

McManus, J.F., Oppo, D.W., Cullen, J.L., 1999. A 0.5-million-year record of millennial-scale climate variability in the North Atlantic. Science 283, 971–975.

Mix, A.C., 1987. The oxygen-isotope record of glaciation. In: Ruddiman, W.F., Wright, H.E.J. (Eds.), North America and Adjacent Oceans during the Last Glaciation. Geol. Soc. Am., Boulder, CO, pp. 111–135.

Molfino, B., Kipp, N.G., Morley, J.J., 1982. Comparison of foraminiferal, coccolithophorid and radiolarian paleotemperature equations: Assemblage coherency and estimate concordancy. Quat. Res. 17, 279–313.

Müller, A., 2000. Mg/Ca and Sr/Ca-Verhältnisse in biogenem

carbonat planktischer Foraminiferen und bentischer Ostracoden. Berichte aus dem Institut für Meereskunde 313, Christian-Albrechts-University, Kiel (in German).

Niebler, H.-S., Gersonde, R., 1998. A planktic foraminiferal transfer function for the southern South Atlantic Ocean. Mar. Micropaleontol. 34, 213–234.

Nürnberg, D., Bijma, J., Hemleben, C., 1996. Assessing the reliability of magnesium in foraminiferal calcite as a proxy for water mass temperatures. Geochim. Cosmochim. Acta 60, 803–814.

Nürnberg, D., Müller, A., Schneider, R.R., 2000. Paleo-sea surface temperature calculations in the equatorial east Atlantic from Mg/Ca ratios in planktic foraminifers: A comparison to SST estimates from $U_{37}^{K'}$ and transfer function. Paleoceanography 15, 124–134.

Oppo, D.W., Lehmann, S.J., 1995. Suborbital timescale variability of North Atlantic Deep Water during the past 200,000 years. Paleoceanography 10, 901–910.

Ottens, J.J., 1992. Planktic foraminifera as indicators of ocean environments in the northeast Atlantic. Ph.D. Thesis, Enschede.

Overpeck, J.T., Webb, T., III, Prentice, I.C., 1985. Quantitative Interpretation of fossil pollen spectra: Dissimilarity coefficients and the method of modern analogs. Quat. Res. 23, 87–108.

Pahnke, K., Zahn, R., Elderfield, H., Schulz, M., 2003. 340,000-year centennial-scale marine record of southern hemisphere climatic oscillation. Science 301, 948–952.

Pflaumann, U., Duprat, J., Pujol, C., Labeyrie, L.D., 1996. SIMMAX: A modern analog technique to deduce Atlantic sea surface temperatures from planktonic foraminifera in deep-sea sediments. Paleoceanography 11, 15–35.

Prell, W.L., 1985. The stability of low latitude sea surface temperatures: An evaluation of the CLIMAP reconstruction with emphasis on positive SST anomalies. Rep. TR 025. U.S. Dept. of Energy, Washington, DC.

Rahmstorf, S., 1995. Bifurcations of the Atlantic thermohaline circulation in response to changes in the hydrological cycle. Nature 378, 145–149.

Ruddiman, W.F., 1977. Late Quaternary deposition of ice-rafted sand in the subpolar North Atlantic (lat. 40° to 65°N). Geol. Soc. Am. Bull. 88, 1813–1821.

Ruddiman, W.F., McIntyre, A., 1976. Northeast Atlantic paleoclimatic changes over the past 600,000 years. Geol. Soc. Am. Mem. 145, 155–173.

Ruddiman, W.F., McIntyre, A., 1984. Ice-age thermal response and climatic role of the surface Atlantic Ocean, 40°N to 63°N. Geol. Soc. Am. Bull. 95, 381–396.

Ruddiman, W.F., Raymo, M.E., McIntyre, A., 1986a. Matuyama 41,000-year cycles: North Atlantic Ocean and northern hemisphere ice sheets. Earth Planet. Sci. Lett. 80, 117–129.

Ruddiman, W.F., Shackleton, N.J., McIntyre, A., 1986. North Atlantic sea-surface temperatures for the last 1.1 million years. In: Summerhayes, C.P., Shackleton, N.J. (Eds.), North Atlantic Paleoceanography. Geol. Soc. Am. Spec. Publ., pp. 155–173.

Saito, T., Thompson, P.R., Breger, D., 1981. Systematic Index of Recent and Pleistocene Planktonic Foraminifera. University of Tokyo Press, Tokyo.

Sarnthein, M., Stattegger, K., Dreger, D., Erlenkeuser, H., Grootes, P., Haupt, B.J., Jung, S., Kiefer, T., Kuhnt, W., Pflaumann, U., Schäfer-Neth, C., Schulz, H., Schulz, M., Seidov, D., Simstich, J., van Kreveld, S., Vogelsang, E., Völker, A., Weinelt, M., 2001. Fundamental modes and abrupt changes in North Atlantic circulation and climate over the last 60 ky - Concepts, Reconstruction and Numerical Modeling. In: Schäfer, P., Ritzrau, U., Schlüter, M., Thiede, J. (Eds.), The Northern North Atlantic: A Changing Environment. Springer, Berlin, pp. 365–410.

Schiebel, R., Bijma, J., Hemleben, C., 1997. Population dynamics of the planktic foraminifer *Globigerina bulloides* from the eastern North Atlantic. Deep-Sea Res. 44, 1701–1713.

Seidov, D., Maslin, M., 1999. North Atlantic deep water circulation collapse during Heinrich events. Geology 27, 23–26.

Shackleton, N.J., 2000. The 100,000-year ice-age cycle identified and found to lag temperature, carbon dioxide, and orbital eccentricity. Science 289, 1897–1902.

Stewart, I.A., Darling, K.F., Kroon, D., Wade, C.M., Troelstra, S.R., 2001. Genotypic variability in subarctic Atlantic planktic foraminifera. Mar. Micropaleontol. 43, 143–153.

van Kreveld, S., Sarnthein, M., Erlenkeuser, H., Grootes, P., Jung, S., Nadeau, M.J., Pflaumann, U., Voelker, A., 2000. Potential links between surging ice sheets, circulation changes, and the Dansgaard-Oeschger cycles in the Irminger Sea, 60-18 kyr. Paleoceanography 15, 425–442.

Venz, K.A., Hodell, D.A., Stanton, C., Warnke, D.A., 1999. A 1.0 Myr record of glacial North Atlantic Intermediate Water variability from ODP site 982 in the northeast Atlantic. Paleoceanography 14, 45–52.

Waelbroeck, C., Labeyrie, L., Duplessy, J.-C., Guiot, J., Labracherie, M., Leclaire, H., Duprat, J., 1998. Improving past sea surface temperature estimates based on planktonic fossil faunas. Paleoceanography 13, 272–283.

Winograd, I.J., Tyler, B.C., Landwehr, J.M., Riggs, A.C., Ludwig, K.R., Szabo, B.J., Kolesar, P.T., Revesz, K.M., 1992. Continuous 500,000-year climate record from vein calcite in Devils Hole, Nevada. Science 258, 255–260.